



**HAL**  
open science

## Comparative study between laboratory and large pilot scales for VOC's removal from gas streams in continuous flow surface discharge plasma

Aymen Amine Assadi, Abdelkrim Bouzaza, Dominique Wolbert

### ► To cite this version:

Aymen Amine Assadi, Abdelkrim Bouzaza, Dominique Wolbert. Comparative study between laboratory and large pilot scales for VOC's removal from gas streams in continuous flow surface discharge plasma. Chemical Engineering Research and Design, 2016, 106, pp.308-314. 10.1016/j.cherd.2015.12.025 . hal-01256845

**HAL Id: hal-01256845**

**<https://univ-rennes.hal.science/hal-01256845>**

Submitted on 24 Mar 2016

**HAL** is a multi-disciplinary open access archive for the deposit and dissemination of scientific research documents, whether they are published or not. The documents may come from teaching and research institutions in France or abroad, or from public or private research centers.

L'archive ouverte pluridisciplinaire **HAL**, est destinée au dépôt et à la diffusion de documents scientifiques de niveau recherche, publiés ou non, émanant des établissements d'enseignement et de recherche français ou étrangers, des laboratoires publics ou privés.

1 **Highlights**

2

3 The removal of isovaleraldehyde by surface plasma discharge was studied

4 Operating parameters are tested at pilot scale with high flow rate

5 The scale-up of plasma reactors were discussed

6 Plasma process was successfully extrapolated at larger scale.

7

8

# Comparative study between laboratory and large pilot scales for VOC's removal from gas streams in continuous flow surface discharge plasma

ASSADI Aymen Amine <sup>a,b</sup>, BOUZAZA Abdelkrim <sup>a,b\*</sup>, WOLBERT Dominique <sup>a,b</sup>,

<sup>a</sup> Laboratoire Sciences Chimiques de Rennes - équipe Chimie et Ingénierie des Procédés, UMR 6226 CNRS, ENSCR-11, allée de Beaulieu, CS 508307-35708 Rennes, France.

<sup>b</sup> Université Européenne de Bretagne, Rennes-France

\* Corresponding author. Tel.: +33 2 23238056; fax: +33 2 23238120.

E-mail address: [Abdelkrim.bouzaza@ensc-rennes.fr](mailto:Abdelkrim.bouzaza@ensc-rennes.fr) (A. BOUZAZA).

## Abstract

This work investigated the performance of Isovaleraldehyde (3-methylbutanal) removal from gas streams using continuous flow surface discharge plasma at room temperature. The feasibility of pollutant removal using up-scaled reactor was systematically assessed by monitoring removal efficiency and mineralization at different operational parameters, such as specific energy, air flow rate and inlet concentration. Results show that increasing flow rate lead to improve the removal capacity. For example, when flow rate extends two times, the removal capacity varies from 0.6 to 1.1 g.h<sup>-1</sup>. Moreover, when specific energy increased, both removal capacity and mineralization were enhanced. Additionally, a comparison between laboratory and pilot scales using surface discharge plasma system was carried out. A methodology of scaling up the surface discharge plasma system was proposed. In this context, removal capacities were compared for different continuous reactors: two reactors at laboratory scale (planar and cylindrical reactor), and pilot unit. The results suggest that the plasma reactor scale-up for pollutant removal can be feasible.

## Keywords

Scaling-up, Continuous reactor, surface discharge plasma, VOCs treatment, byproducts

## Introduction

Volatile organic compounds (VOCs) had adverse effects on environment and human health. They are emitted from different outdoor sources (motor vehicles, incomplete combustion in industrial processes) (Le Cloirec, 1998) as well as from indoor sources (ADEME, 2005). Various methods have been developed for indoor air cleaning and VOCs

42 removal such as thermal and catalytic incineration (Li and Gong, 2010), absorption (Hsu  
43 and Lin, 2011), adsorption (Kim and Ahn, 2012), condensation (Tan et al., 2005),  
44 biofiltration (Zehraoui et al., 2012), ozonation (Ogata et al., 2010) and photocatalysis  
45 (Hussain et al., 2011; Assadi et al., 2012). Although several chemical methods were used  
46 or studied for the effective treatment of VOCs, the environmental applications of non-thermal  
47 plasma (NTP) started at the **beginning of the XX<sup>th</sup> century** with the use of plasma-generated  
48 ozone for water depollution. Later on, this type of treatment process was successfully  
49 developed for air treatment (Khacef et al., 2006).

50 The most significant advantage of NTP generated in ambient air **was the production** of  
51 highly reactive oxidizing radicals such as O<sup>°</sup> and HO<sup>°</sup>, and also O<sub>3</sub>. **Such species were**  
52 **produced at room temperature** and at low energy cost compared to any alternative methods  
53 (Malik et al., 2011; Nunez et al., 1993). As a result, non-thermal plasma **could easily break**  
54 most chemical bonds of molecular pollutants at low temperatures and convert gas pollutants  
55 into end-products including CO, CO<sub>2</sub>, H<sub>2</sub>O (Cho et al., 2012). On the other hand, many  
56 researches on NTP technologies for processing gases **show that NTP is very effective for**  
57 **gas treatment at low VOCs concentrations** (Kim, 2004; Hammer, 2014). In fact, our  
58 previous **research proved that** some VOCs in gas streams can be degraded efficiently by  
59 surface discharge plasma at laboratory scale pilots with two different geometries (Assadi et  
60 al., 2014a).

61 This present paper was to extend previous research at lab scale (Assadi et al., 2014a; Assadi  
62 et al., 2014b) by adding a new investigation about pilot scale of surface plasma application.  
63 Moreover, a special attention **was given to high** flow rate parameter (from 250 to 500 m<sup>3</sup>.h<sup>-1</sup>)  
64 and its effect on the reactor performance, which is innovative in comparison to the latter  
65 studies. **Here, isovaleraldehyde (isoval)** was chosen since this pollutant was the main  
66 molecule detected in the exhaust gases from animal quartering centers (ADEME, 2005).  
67 Another goal of the present work is to investigate **different reactors scales** (laboratory and  
68 pilot) in order to see the **possibility of the scale-up of the process**.

69

## 70 2. Experimental setup

71

72 The used experimental setup **was structured as follows**: (i) continuous reactors, (ii) plasma  
73 system and (iii) analysis set-up.

74

75 **2.1. Plasma reactors**

76

77 **2.1.1. Laboratory reactors**

78

79 The experiments were carried out in ambient conditions, i.e. room temperature and pressure.

80 **Two lab scale reactors were tested. The first one, planar reactor, consisted** of a  
81 rectangular cross section (135 mm × 135 mm) and is 1 m length. **It contained two plates**, 4  
82 mm thickness, **which were arranged parallel to** the length of the reactor and permit to hold  
83 up the two **electrodes (Fig.1b)**. **The second one, cylindrical reactor, was composed**  
84 principally of a glass tube (58 mm id and 100 cm length). It was covered by a copper grid  
85 forming the outer electrode. The glass tube, 4 mm thickness, acts as the dielectric media. The  
86 High Voltage (HV) **electrode was a helicoidally** wire shaped as a coil spring in close contact  
87 with the inner wall of the reactor (Fig. 1a). A detailed description of the geometry of the  
88 plasma reactor and electrical measurements **was published elsewhere (Guillerm et al.,**  
89 **2014)**.

90

91 **Fig1: Scheme and sectional drawing of the cylindrical (a) and planar (b) reactors**

92

93 **2.1.2. Pilot unit**

94

95 **This reactor was an air** handling unit produced by CIAT (Compagnie Industrielle  
96 d'Applications Thermiques- France) with a flow rate capacity up to 5000 m<sup>3</sup>.h<sup>-1</sup> (**Figure2**).  
97 The unit comprised a pre-filtration box, a cooling bank, an electric heater (box no. 1), a vapor  
98 humidifier (box no. 2), a pollutant injection area (box no. 3), an upstream pollution  
99 measurement box, a surface plasma treatment system, a downstream concentration  
100 measurement box (box no. 4); a fan (box no. 5) and finally an activated carbon filtration (box  
101 no. 6). **The ventilation box consisted** of a medium-pressure centrifugal fan. **The used pilot**  
102 **was described in detail in our previous work (Assadi et al., 2014c)**.

103

104 **Figure 2: A functional diagram of pilot unit supplied by CIAT**

105

## 106 **2.2. Plasma system**

107

108 **The experimental set-up for surface discharge production was similar to the planar**  
109 **reactor. In fact, one side of the partition was provided with metallic grid forming the**  
110 **HV electrode. The total surface area of each lab reactor was  $0.18\text{m}^2$ . As seen in figure 3,**  
111 **the other side was formed of a copper sheet that served as a ground electrode. The two**  
112 **electrodes were separated by a dielectric sheet of glass (thickness 4 mm). These elements**  
113 **were tied together and this configuration was reproduced six times forming six parallel**  
114 **channels. The polluted gas flowed through these channels. The details concerning the**  
115 **surface discharge plasma system of the pilot unit were shown in figure 3.**

116

117 **Figure 3: Photography of Plasma system used in pilot unit**

118

119 The surface discharge **was obtained** by submitting the electrodes to a sinusoidal high voltage  
120 ranging from 0 to 30 kV (peak to peak) at 50 Hz frequency. The outer electrode **was**  
121 **connected to the ground through** a 50 nF of capacity in order to collect the charges  
122 transferred through the reactor. The applied voltage ( $U_a$ ) and high capacitance **voltage ( $U_m$ )**  
123 **were measured by LeCroy high voltage probes and recorded by digital oscilloscope (Lecroy**  
124 **Wave Surfer 24 Xs, 200 MHz).**

125 The air-isovaleraldehyde gas mixture was prepared by passing synthetic air (Air Liquide)  
126 through liquid isovaleraldehyde (Sigma-Aldrich, 97%). **In fact, the pollutant (liquid) was**  
127 **firstly pressurized** with air in a stainless steel tank (500 mL). Then, it was heated, vaporized  
128 and mixed with a zero-air flow in an especially designed Bronkhorst vaporization/mixing  
129 chamber (CEM). In these conditions, **the inlet concentrations ranged from 2 to  $10\text{mg}\cdot\text{m}^{-3}$ .**

130

## 131 **2.3. Analysis set-up**

132

133 **The experiment was carried out at room temperature and atmospheric pressure. The**  
134 **temperature and relative humidity were measured by a TESTO sensor.** The gases (direct  
135 sampling or after concentration) were analysed by means of gas chromatography with a flame

136 ionisation detector (FID) or mass spectrometry (MS). CO and CO<sub>2</sub> **analysers were used to**  
 137 **monitor the carbon monoxide and dioxide. Ozone formed in the plasma reactor was measured**  
 138 **by bubbling it through a suitable liquid phase of KI. The analysis system was largely**  
 139 **described in previous studies (Assadi et al., 2012, 2013 and 2014a).**

### 140 3. Results and discussion

141

142 **Experimental parameters were defined as follows: ( $C_{in}$ ) and ( $C_{out}$ ) represented inlet and**  
 143 **outlet concentration of pollutant ( $\text{mg}/\text{m}^3$ ) respectively.**

144

145 The specific energy (SE) was defined as the energy deposited per unit volume of the gas flow:

$$146 \quad SE \text{ (J.L}^{-1}\text{)} = P/(Q*1000) \quad (1)$$

147 where P was the input power (W) and Q denoted the total gas flow rate ( $\text{m}^3.\text{s}^{-1}$ ).

148 To evaluate the plasma process, the following parameters are employed:

- 149 • The removal capacity (R) which was calculated from:

$$150 \quad R = Q \cdot \frac{C_{in}}{100} \cdot IRE(\%) \quad (2)$$

151 where IRE(%) isovaleraldehyde removal was defined as

$$152 \quad IRE(\%) = \frac{C_{in} - C_{out}}{C_{in}} \times 100\% \quad (3)$$

- 153 • The energy yield  $\eta_E(\text{eV}/\text{molecule}) = 3.21 \cdot 10^3 * P/[Q * (C_{in} - C_{out})]$  (4)

154 where  $3.21 \cdot 10^3$  was constant taking account Avogadro's number, molecular  
 155 weight of Isoval and joule to electron-volt Conversion.

- 156 • The selectivities of CO and CO<sub>2</sub> which were defined as:

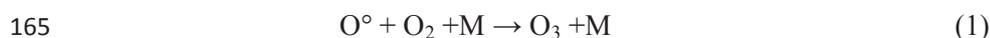
$$157 \quad S_{CO}(\%) = \frac{[CO]}{(5 \times [Isoval]_{conv})} \times 100 \quad (5)$$

158

$$159 \quad S_{CO_2}(\%) = \frac{[CO_2]}{(5 \times [Isoval]_{conv})} \times 100 \quad (6)$$

160 where [CO] and [CO<sub>2</sub>] were respectively the concentrations of carbon monoxide and  
 161 carbon dioxide detected in the effluent gas as a result of Isoval removal, and [Isoval]<sub>conv</sub>  
 162 was the concentration of Isovaleraldehyde converted by plasma surface discharge.

163 • Ozone concentration: Ozone was well known to be an inevitable byproduct in a  
 164 plasma process. **It could be formed by the following** reaction:



166

167 **where O<sup>°</sup> was atomic oxygen and was generated by O<sub>2</sub> dissociation due to its impact**  
 168 **with high energy electrons, and M could be either molecular oxygen or molecular nitrogen**  
 169 **(Atkinson et al., 2003). Moreover, several mechanisms occurred when non-thermal**  
 170 **plasma was present since plasma produces various species such as high energy electrons,**  
 171 **excited molecules or radicals (O<sup>°</sup>, N<sup>\*</sup>, °OH, O<sub>2</sub><sup>-</sup>, O<sub>3</sub>, NO<sub>2</sub>, NO<sub>x</sub>, etc.). These molecules**  
 172 **could interact directly with VOC molecules (Atkinson et al., 2003).**

173

### 174 3.1. Pilot unit efficiency

175

176 **The reactor was already being flushed under surface discharge for 1hour when we**  
 177 **started** sampling for analysis. Indeed, the inlet and outlet gas **were then sampled manually.**  
 178 **The experiments which were repeated two times; showed a good reproducibility with**  
 179 **5% standard** deviation. This standard deviation was represented by vertical bars in the  
 180 experimental results in all figures.

181 Moreover, the performance of pollutant removal using the pilot unit (500 m<sup>3</sup>.h<sup>-1</sup>) was  
 182 systematically assessed by monitoring the removal efficiency, the mineralization and ozone  
 183 formation at different operational parameters, such as specific energy, air flow rate and inlet  
 184 concentration.

#### 185 3.1.1. Removal capacity of Isoval

186

187 The removal capacity of isovaleraldehyde was investigated by studying the effect of specific  
 188 energy, flowrate and inlet concentration of **pollutant (Figure 4.a). Firstly, figure 4.a showed**  
 189 **that the increase of flowrate improved the removal capacity. In fact, at flowrate equal to 250**  
 190 **m<sup>3</sup>.h<sup>-1</sup> and 3 mg.m<sup>-3</sup> of inlet concentration, when SE extended six times, the removal**  
 191 **capacity increased from 0.2 to 0.45 g.h<sup>-1</sup>.** This result was similar to those reported for  
 192 trimethylamine and isovaleric acid at laboratory scale (Assadi et al., 2014a), for toluene  
 193 (Vandenbroucke et al., 2011), H<sub>2</sub>S (Chen and Xie, 2013) and for NO<sub>x</sub> (Khacef et al.,  
 194 2013).. On the other hand, for a selected flow rate, it was interesting to report that  
 195 experimental results showed an enhanced removal capacity when increasing inlet

196 concentration. Similar results were found in previous studies (Assadi et al., 2014a). For  
197 diluted effluent, the oxidation rate was directly proportional to the inlet concentration. The  
198 **degradation occurred to fit a pseudo first-order kinetic**. At this specific concentration  
199 range, many reactive species remained available for the reaction. On the other hand, the  
200 experimental results about the effect of air flow rate (Q) on isovaleraldehyde removal were  
201 illustrated in Fig. 4.a. In our case, despite the decrease of residence time, an improvement in  
202 the removal capacity was noticed. Indeed, at  $SE = 4.5 \text{ J.L}^{-1}$  and when Q increased from 250 to  
203  $500 \text{ m}^3/\text{h}$ , removal capacity increased two times. **The gas-phase mass transfer rate**  
204 **influenced the treatment capacity by producing a concentration gradient between the**  
205 **bulk and the discharge zone. For instance under transitional conditions, the removal**  
206 **capacity depended on gas-phase mass transfer rate and plasma reaction rate (Assadi et**  
207 **al., 2014d). At higher flow rate, the process become a chemically step controlled. Thus, it**  
208 **could be suggested that the increase of air flow was helpful to the transfer of**  
209 **isovaleraldehyde molecules from bulk to discharge zone (Vandenbroucke et al., 2011).**

210

211 **Figure 4.a: Removal capacity of Isoval and energy yield vs. specific energy at different**  
212 **flow rates and different inlet concentrations using pilot unit.**

213

214 **However, in practice, energy cost  $\eta_E$  (eV/molecule) is an important parameter; the**  
215 **variation of this parameter with different operating parameters was shown in figure 4.b.**  
216 **In fact, the energy cost for conversion was higher for lower isoval initial concentrations,**  
217 **exceeding  $2.9 \text{ keV/molecule}$  for the lowest concentration investigated ( $3 \text{ mg/m}^3$ ). On the**  
218 **other hand, we noted that energy cost was flow rate independent because when we**  
219 **increased the flow rate we must increase also the power in order to keep SE constant.**

220

221 **Figure 4.b: Energy yield vs specific energy at different flow rates and different inlet**  
222 **concentrations using pilot unit**

223

### 224 **3.1.2. By-products formation**

225

226 **At pilot scale, the detected by-products were acetone ( $\text{CH}_3\text{COCH}_3$ ), acetic acid**  
227 **( $\text{CH}_3\text{COOH}$ ), CO and  $\text{CO}_2$ . We note that these by-products were similar to those seen at**

228 **lab scale.** A possible **pathway of Isoval removal** was proposed in our previous  
229 investigation with cylindrical reactor at lab scale (Assadi et al., 2014e).

230

### 231 3.1.2.1. CO and CO<sub>2</sub> formation

232

233 When increasing the specific energy, **the discharges snatched more** electrons from the gas-  
234 phase inducing a higher concentration of reactive species in the plasma (Fig.5). So, more  
235 reactive **species were available to induce by-product** mineralization. **Same results were**  
236 **reported in other studies** at laboratory scale (Lee et al., 2014; Zhang et al., 2014; Xiao et  
237 al., 2014). **It was well known that at** laboratory scale, the decrease of flow rate and inlet  
238 concentration lead to an increase of mineralization.

239

240 **Figure 5: Variation of the mineralization vs. specific energy at different inlet**  
241 **concentrations and different flow rates**

242

243 **Fig.6 depicted the effect** of specific energy, flow rate and inlet concentration of CO  
244 selectivity. **It was interesting** to note that whatever the experimental conditions used,  
245 experimental **results showed that CO** selectivity was **globally not dependent upon the inlet**  
246 **concentration** and flow rate **and it didn't exceed** 15 %. This effect could be due to tested  
247 concentrations interval which was very low. So, the effect of these two parameters was not  
248 significant. **Previous studies were shown that with surface plasma discharge, the**  
249 **selectivity of CO was widely specific energy dependent** (Thevenet et al., 2014; Assadi et  
250 al., 2014e).

251

252 **Figure 6: Variation of the CO selectivity (%) vs. specific energy at different inlet**  
253 **concentrations and different flow rates.**

254

### 255 3.1.2.2. Ozone formation

256

257 **Fig. 7 showed** the variation of O<sub>3</sub> concentration with specific energy at different inlet  
258 concentration and different flow rates. First of all, it was well known that at laboratory scale,  
259 the increase of **specific energy leaded to an increase of ozone concentration.** **The behavior**  
260 **with pilot scale was similar to that was seeing at lab scale.** In fact, increasing two times the

261 specific energy led to an increase of the concentration of formed ozone by 5 ppm.  
262 Additionally, at  $Q= 250 \text{ m}^3.\text{h}^{-1}$ , the highest ozone concentrations were obtained at low inlet  
263 concentration. This suggests, when compared with previous studies, especially with the planar  
264 reactor, that the reactive species such as active atomic oxygen and  $\text{O}_3$  would also be  
265 consumed to react with isovaleraldehyde or by-products (Thevenet et al., 2014). Thus, the  
266 consumption of active species such as O could explain the decreasing ozone concentration in  
267 the presence of high inlet concentration of Isoval (Reaction 1).

268 **Moreover, ozone increased with the increase of flow rate. In fact, active species usually**  
269 **reacted with VOC present in gas. The decrease of the residence time reduced the active**  
270 **species/VOC contact probability, allowing an important recombination reaction**  
271 **(Reaction1.)**

272

273 **Figure 7: Variation of the ozone vs. specific energy at different inlet concentrations and**  
274 **different flow rates**

275

### 276 **3.2. Comparison of reactors**

277

278 **In the next step of this investigation, we compared results obtained** at lab scale with the  
279 removal capacity of pilot unit. A methodology **was proposed to scale-up surface** discharge  
280 reactors, employing purely laboratory information, avoiding the need of using adjustable  
281 parameters for each different application of the same process. For this purpose,  
282 isovaleraldehyde removal was studied previously in a laboratory scale reactor.

283 As explained above, under our experimental conditions, many parameters **were kept the**  
284 **same** for the two reactors studied: residence time, feed of Isoval (flow rate  $\times$  inlet  
285 concentration), relative humidity and temperature. Indeed, feed of Isoval and residence times  
286 for lab and pilot scale were kept constant and equal to  $1.2 \text{ g}.\text{h}^{-1}$  and  $0.6\text{s}$  respectively ( $4 \text{ m}^3.\text{h}^{-1}$   
287 for the cylindrical reactor,  $10 \text{ m}^3.\text{h}^{-1}$  for the planar reactor and  $250 \text{ m}^3.\text{h}^{-1}$  for pilot unit).

288 **Figure 8 showed the removal capacities** of Isoval using different scale reactors. The results  
289 showed that **the removal capacities with Pilot scale were about six times higher than that**  
290 **of the laboratory reactors, regarding to flow rate and plasma surface involved.**  
291 **Moreover, at high value of flow rate, the mass transfer was not a limited step.** Thus,  
292 previous results and present study confirmed that the scale-up of the surface discharge plasma

293 could have been possible from the laboratory reactor study. **This study showed that** data  
294 obtained for surface plasma process at laboratory scale can be used for industrial design.

295

296 **Figure 8: Different reactors and scales comparison vs. specific energy: Feed of Isoval =**  
297 **1.2 g.h<sup>-1</sup>, residence time=0.6s**

298

#### 299 **4. Conclusion**

300

301 The removal of **isovaleraldehyde was carried** out on surface discharge at pilot scale with  
302 high flow rates.

303 The results showed that the increment's effect of specific energy seemed to be significant on  
304 the average removal capacity and on the overall selectivity to CO<sub>2</sub>. Additionally, the increase  
305 **of flow rate led to improve the** removal of pollutant due to enhancement of mass transfer  
306 step.

307 The removal capacities of isovaleraldehyde with three different scale reactors were compared  
308 and the feasibility of the scale-up process **was demonstrated due** to continuity of the  
309 experimental results obtained. Thus, **the present study confirmed** that the scale-up of the  
310 surface discharge plasma could have been possible from the laboratory reactor study. Thus, an  
311 industrial design of plasma reactor **could be possible** by using only data lab.

312

#### 313 **Acknowledgment**

314

315 The authors gratefully acknowledged the financial support provided by the French National  
316 Research Agency (ANR) for this research work.

317

318

319

320

321

322

323

324 **References**

325

326 ADEME, Pollutions olfactives : origine, législation, analyse, traitement. Ademe, Dunod,  
327 Angers, 2005.

328 Aerts R., Tu X., Van Gaens W., Whitehead J. C., Bogaerts A., Gas Purification by Nonthermal  
329 Plasma: A Case Study of Ethylene, **Environmental Science & Technology**. 47 (2013)  
330 6478–6485

331 Atkinson R., Baulch D. L., Cox R. A., Crowley J. N., Hampson R. F., Hynes R. G., Jenkin M.  
332 E., Rossi M. J., Troe J., Evaluated kinetic and photochemical data for atmospheric chemistry:  
333 Part 1 - gas phase reactions of Ox, HOx, NOx and SOx species. *Atmospheric chemistry and*  
334 *Physics Discussions* 3 (2003) 6179–6699.

335 Assadi A.A., Bouzaza A., Lemasle M., Wolbert D., Removal of trimethylamine and isovaleric  
336 acid from gas streams in a continuous flow surface discharge plasma reactor, **Chemical**  
337 **Engineering Research And Design** 93 (2015) 640–651.

338 Assadi A. A., Palau J., Bouzaza A., Peña-Roja J., Martínez-Soria V., Wolbert D., Abatement  
339 of 3-methylbutanal and trimethylamine with combined plasma and photocatalysis in a  
340 continuous planar reactor, *Journal of Photochemistry and Photobiology A: Chemistry* 282  
341 (2014 b) 1–8.

342 Assadi A.A., Bouzaza A., Wolbert D., Petit P., Isovaleraldehyde elimination by UV/TiO<sub>2</sub>  
343 **photocatalysis: comparative study of the process at different reactors configurations and**  
344 **scales, Environmental Science and Pollution Research** 21 (2014 c) 11178-11188

345 Assadi A. A., Bouzaza A., Merabet S., Wolbert D., Modeling and simulation of VOCs  
346 removal by nonthermal plasma discharge with photocatalysis in a continuous reactor:  
347 Synergetic effect and mass transfer, *Chemical Engineering Journal* 258 (2014 d) 119–127.

348 Assadi A. A., Bouzaza A., Vallet C., Wolbert D., Use of DBD plasma, photocatalysis, and  
349 combined DBD plasma/photocatalysis in a continuous annular reactor for isovaleraldehyde  
350 elimination – Synergetic effect and byproducts identification, *Chemical Engineering Journal*  
351 254 (2014 e) 124–132.

352

353 Bahri M., Haghghat F., Plasma-Based Indoor Air Cleaning Technologies: The State of the  
354 Art-Review, *Clean – Soil, Air, Water* 42 (2014), 1667–1680

355 Brandenburg R., Kovacevic V. V., Schmidt M., Basner R., Kettlitz M., Sretenovic  
356 G.B., Obradovic B.M., Kuraica M.M., Weltmann K.-D., Plasma-Based Pollutant Degradation  
357 in Gas Streams: Status, Examples and Outlook, *Contributions to Plasma Physics*, 54 (2014)  
358 202 – 214

- 359 Chen J., XieZh., Removal of H<sub>2</sub>S in a novel dielectric barrier discharge reactor with  
360 photocatalytic electrode and activated carbon fiber. *Journal of Hazardous Materials* 261  
361 (2013) 38–43
- 362 Guillerm M., Assadi A. A., Bouzaza A., Wolbert D., Removal of gas-phase ammonia and  
363 hydrogen sulfide using photocatalysis, nonthermal plasma, and combined plasma and  
364 photocatalysis at pilot scale, ***Environmental Science and Pollution Research***, 21 (2014)  
365 13127-13137
- 366 Gumuchiana D., Cavadias S., Dutenc X., Tatouliana M., Da Costa P., Ognier S., Organic  
367 pollutants oxidation by needle/plate plasma discharge: On the influence of the gas nature,  
368 *Chemical Engineering and Processing* 82 (2014) 185–192.
- 369 Gupta V.K., Verma N., Removal of volatile organic compounds by cryogenic condensation  
370 followed by adsorption. ***Chemical Engineering Science*** 57(2002) 2679–2696.
- 371 Hammer Th., Atmospheric Pressure Plasma Application for Pollution Control in Industrial  
372 Processes, ***Contributions to Plasma Physics***. 54 ( 2014) 187 – 201.
- 373 Hussain M., Russo N., Saracco G., Photocatalytic abatement of VOCs by novel optimized  
374 TiO<sub>2</sub> nanoparticles. *Chemical Engineering Journal* 166(2011)138–149
- 375 Hsu L.J., Lin C.C. Removal of methanol and 1-butanol from binary mixtures by absorption  
376 in rotating packed beds with blade packings, *Chemical Engineering Journal*, 168 (2011)190–  
377 200
- 378 Khacef A.; Cormier J.- M., Pulsed sub-microsecond dielectric barrier discharge treatment of  
379 flue gas simulated glass manufacturing industry: Removal of SO<sub>2</sub> and NO<sub>x</sub>, *Journal of*  
380 *Physics D: Applied Physics*, 39 (2006) 1078-1083
- 381 Khacef A., Da Costa P., Djéga-Mariadassou G., Plasma Assisted Catalyst for NO<sub>x</sub>  
382 Remediation from Lean Gas Exhaust, *Journal of Engineering and Technology research*, 1  
383 (2013) 112-122.
- 384 Kim H., Nonthermal Plasma Processing for Air-Pollution Control: A Historical Review,  
385 Current Issues, and Future Prospects, ***Plasma Processes and Polymers***. 1 (2004) 91–110.
- 386 Kim K.J., Ahn H.G., The effect of pore structure of zeolite on the adsorption of VOCs and  
387 their desorption properties by microwave heating. ***Microporous and Mesoporous Materials***  
388 152 (2012)78–83
- 389 Le Cloirec P., 1998. Les composés organiques volatils dans l'environnement, Lavoisier, Paris.
- 390 Lee H., Lee D.-H., Song Y.-H., Choi W. Ch., Park Y.-K., Kim D. H., Synergistic effect of  
391 non-thermal plasma-catalysis hybrid system on methane complete oxidation over Pd-based  
392 catalysts, ***Chemical Engineering Journal*** 259 (2015) 761–770
- 393 Li W.B., Gong H., Recent progress in the removal of volatile organic compounds by  
394 catalytic combustion. ***Acta Physico-Chimica Sinica*** 26(2010) 885–894

- 395 Malik M. A., Kolb J. F., Sun Y., Schoenbach K.H., Comparative study of NO removal in  
396 surface-plasma and volume-plasma reactors based on pulsed corona discharges, *Journal of*  
397 *Hazardous Materials* 197 (2011) 220–228.
- 398 Nunez C.M., Ramsey G.H., Ponder W.H., Abbott J.H., Hamel L.E., Kariher P.H. (1993)  
399 Corona destruction: an innovative control technology for VOCs and air toxics. ***Journal of Air***  
400 ***& Waste Management* 43(1993) 242–247.**
- 401 Ogata A., Saito K., Kim H-H, Sugawara M., Aritani H., Einaga H., Performance of an  
402 Ozone Decomposition Catalyst in Hybrid Plasma Reactors for Volatile Organic Compound  
403 Removal, *Plasma Chemistry and Plasma Processing* 30(2010) 33–42.
- 404 Tan S.J., Li L., Xiao Z.Y., Wu Y.T., Zhang Z.B., Pervaporation of alcoholic beverages: the  
405 coupling effects between ethanol and aroma compounds. ***Journal of Membrane Science***  
406 **264(2005) 129–136.**
- 407 Thevenet F., Sivachandiran L., Guaitella O., Barakat C., Rousseau A.: Plasma–catalyst coupling  
408 for volatile organic compound removal and indoor air treatment: a review, ***Journal of Physics***  
409 **D: Applied Physics** 47 (2014) 224011–224022
- 410 **Vandenbroucke A.M., Morent R., De Geyter N., Leys C., Non-thermal plasmas for non-**  
411 **catalytic and catalytic VOC abatement, *Journal of Hazardous Materials* 195 (2011) 30–**  
412 **54.**
- 413 Xiao G., Xu W., Wu R., Ni M., Du Ch., Gao X., Luo Zh., Cen K., Non-Thermal Plasmas for  
414 VOCs Abatement, ***Plasma Chemistry and Plasma Processing*** 34 (2014) 1033–1065.
- 415 Zehraoui A., Hassan A.A., Sorial G.A. Effect of methanol on the biofiltration of n-hexane.  
416 ***Journal of Hazardous Materials* 219 (2012) 176–182**
- 417 Zhang H., Li K., Shu Ch., Lou Z., Sun T., Jia J., Enhancement of styrene removal using a  
418 novel double-tube dielectric barrier discharge (DDBD) reactor, *Chemical Engineering Journal*  
419 256 (2014) 107–118.
- 420
- 421
- 422
- 423
- 424
- 425
- 426
- 427

428

429 **Figures**

430

431 **Fig1: Scheme and sectional drawing of the cylindrical (a) and planar (b) reactors**

432

433 **Figure 2: A functional diagram of pilot unit supplied by CIAT**

434

435 **Figure 3: Photography of Plasma system used in pilot unit**

436

437 **Figure 4.a: Removal capacity of Isoval vs specific energy at different flow rates and**  
438 **different inlet concentrations using pilot unit**

439

440 **Figure 4.b: Energy yield vs specific energy at different flow rates and different inlet**  
441 **concentrations using pilot unit**

442

443 **Figure 5: Variation of the mineralization vs. specific energy at different inlet**  
444 **concentrations and different flow rates**

445

446 **Figure 6: Variation of the CO selectivity (%) vs. specific energy at different inlet**  
447 **concentrations and different flow rates.**

448

449 **Figure 7: Variation of the ozone vs. specific energy at different inlet concentrations and**  
450 **different flow rates**

451

452 **Figure 8: Different reactors and scales comparison vs. power consumption specific**  
453 **energy: Feed of Isoval = 1.2 g.h<sup>-1</sup>, residence time=0.6s**

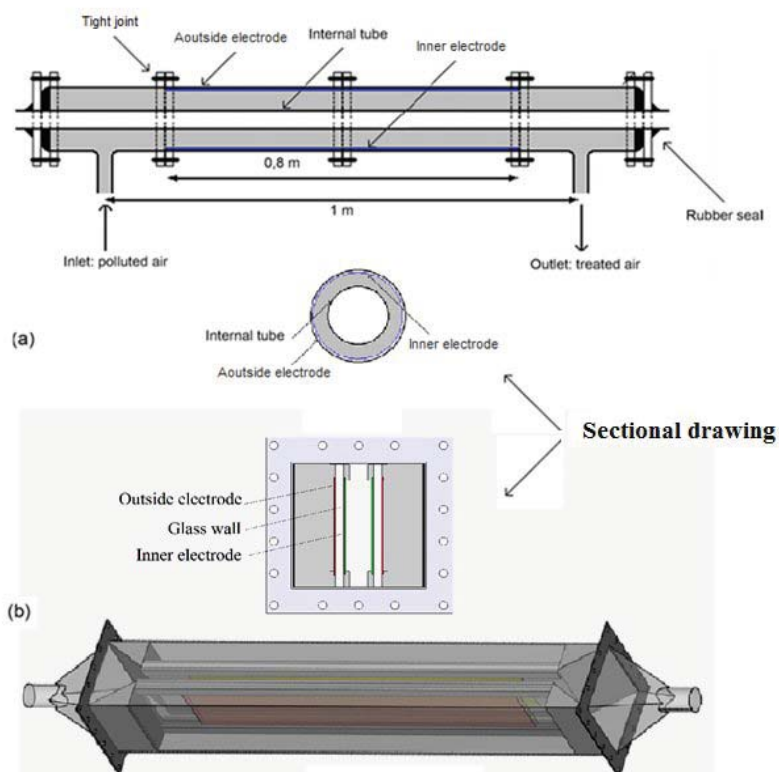
454

455

456

457

458



459

460 **Fig1: Scheme and sectional drawing of the cylindrical (a) and planar (b) reactors**

461

462

463

464

465

466

467

468

469

470

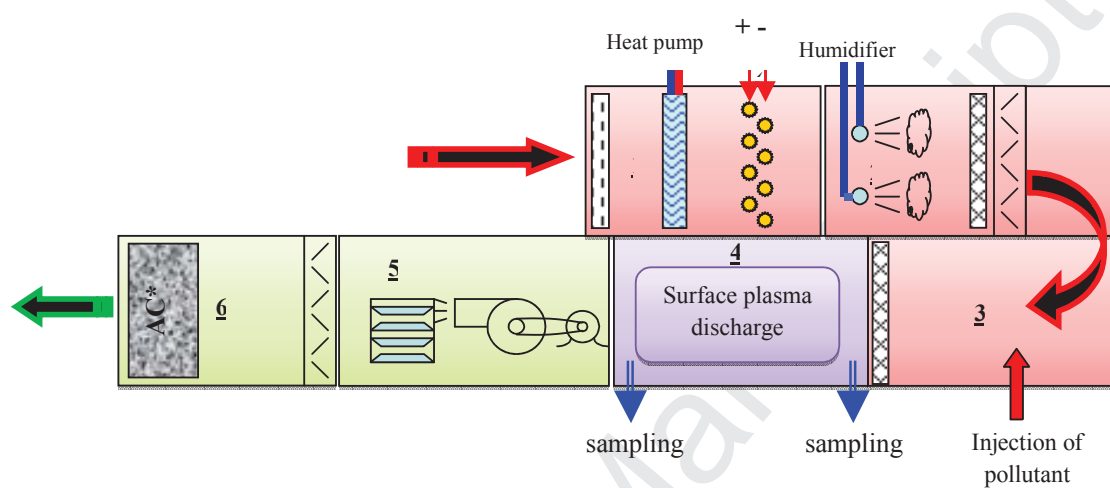
471

472

473

474

475



476

477

478

Figure 2: A functional diagram of pilot unit supplied by CIAT

479

480

481

482

483

484

485

486

487

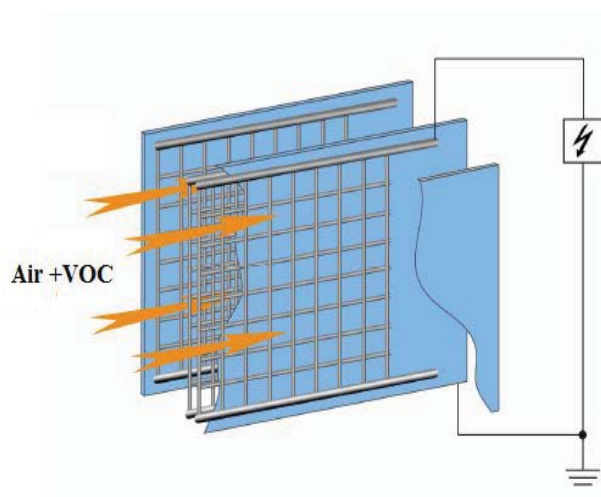
488

489

490

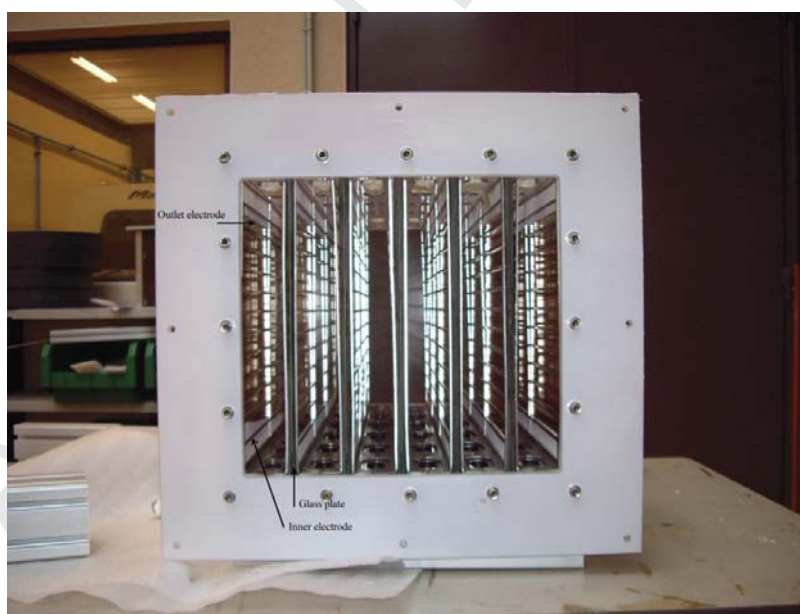
491

492



493

494



495

496

**Figure 3: Photography of Plasma system used in pilot unit**

497

498

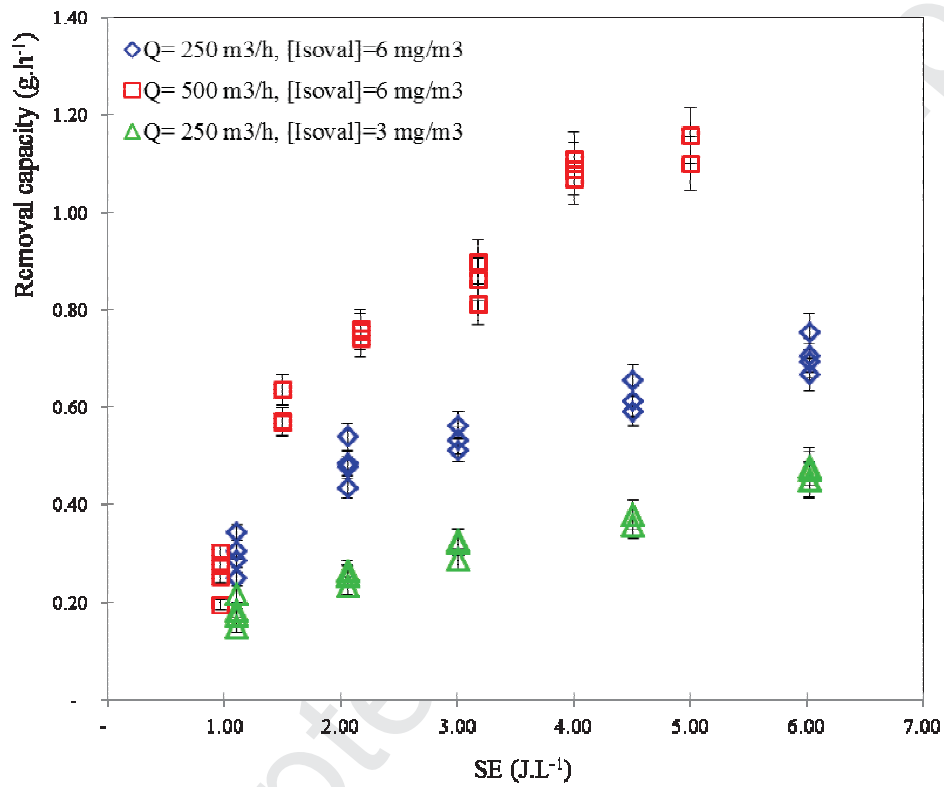
499

500

501

502

503



504

505 **Figure 4.a: Removal capacity of Isoval vs specific energy at different flow rates and**  
506 **different inlet concentrations using pilot unit**

507

508

509

510

511

512

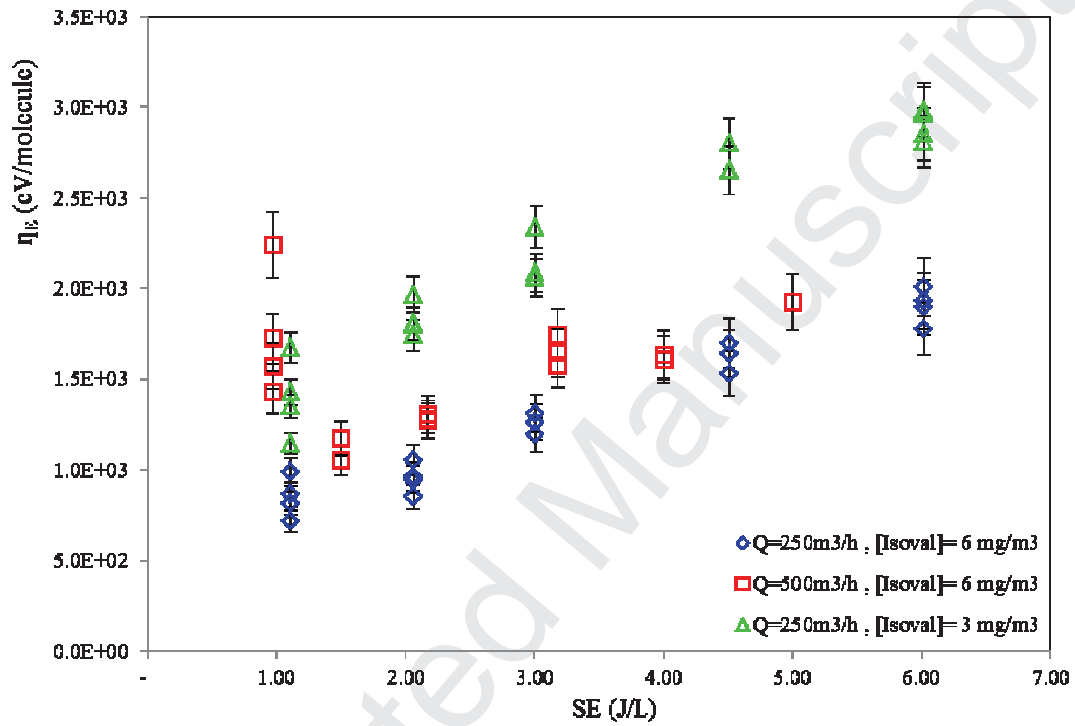
513

514

515

516

517  
518  
519  
520  
521



522  
523  
524  
525  
526  
527  
528  
529  
530  
531  
532  
533  
534  
535  
536

Figure 4.b: Energy yield vs specific energy at different flow rates and different inlet concentrations using pilot unit

537

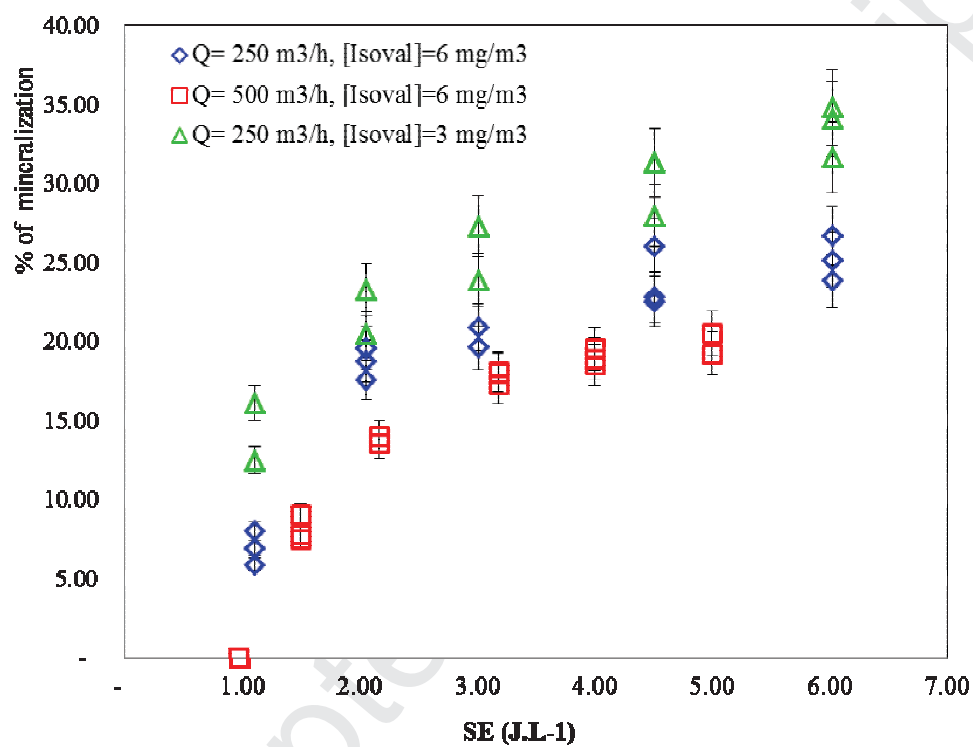
538

539

540

541

542



543

544 **Figure 5: Variation of the mineralization vs. specific energy at different inlet**  
545 **concentrations and different flow rates**

546

547

548

549

550

551

552

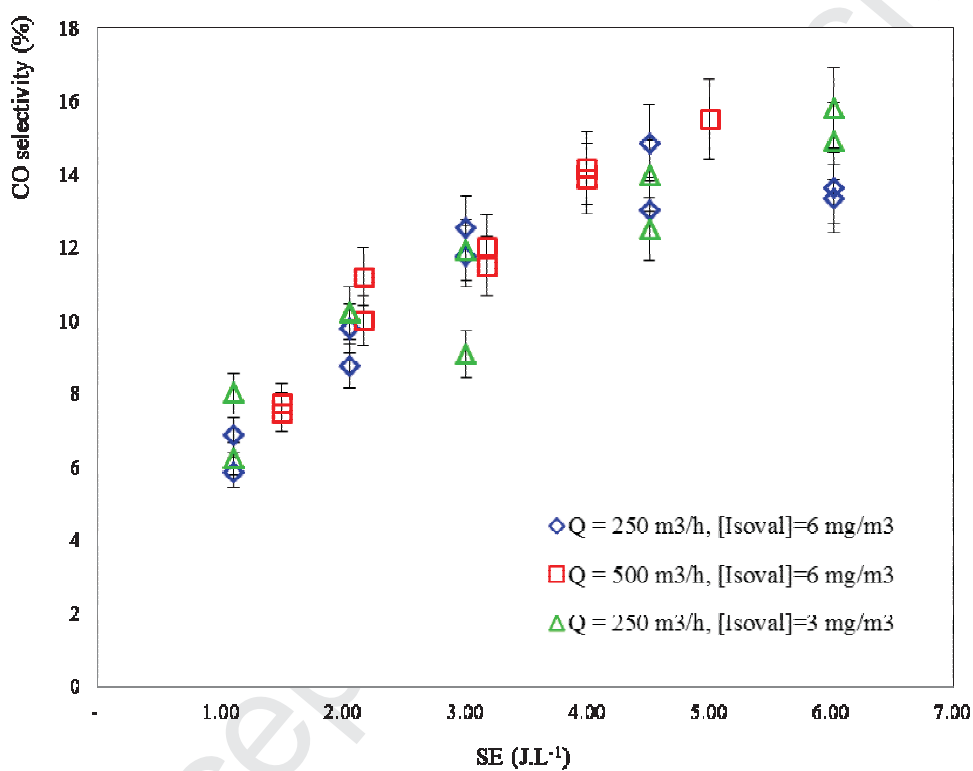
553

554

555

556

557



558

559 **Figure 6: Variation of the CO selectivity (%) vs. specific energy at different inlet**  
560 **concentrations and different flow rates.**

560

561

562

563

564

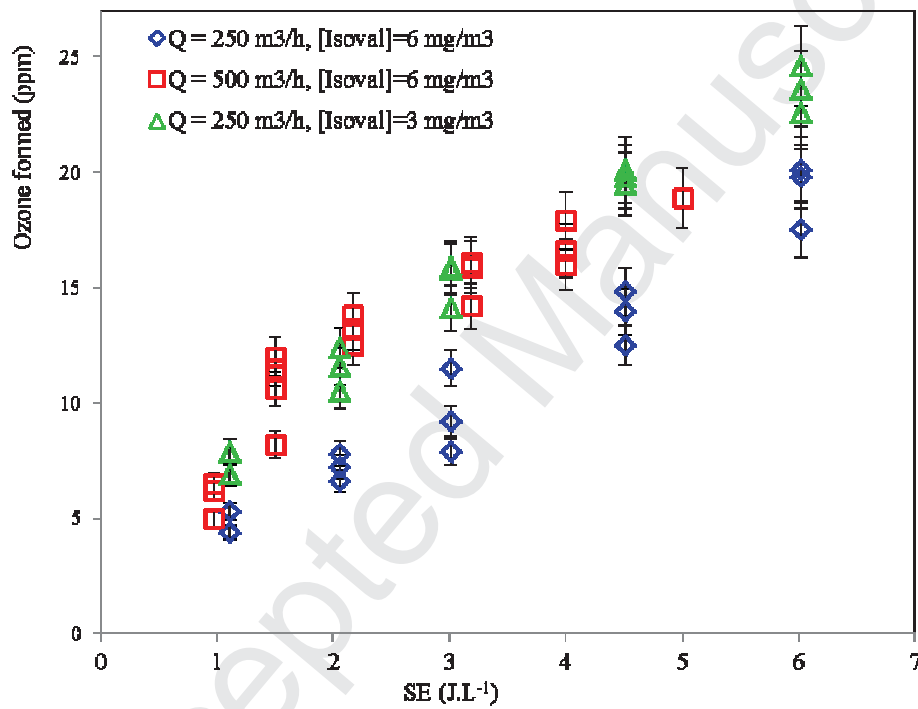
565

566

567

568

569  
570  
571  
572  
573  
574  
575  
576



577

578 **Figure 7: Variation of the ozone vs. specific energy at different inlet concentrations and**  
579 **different flow rates**

580

581

582

583

584

585

586

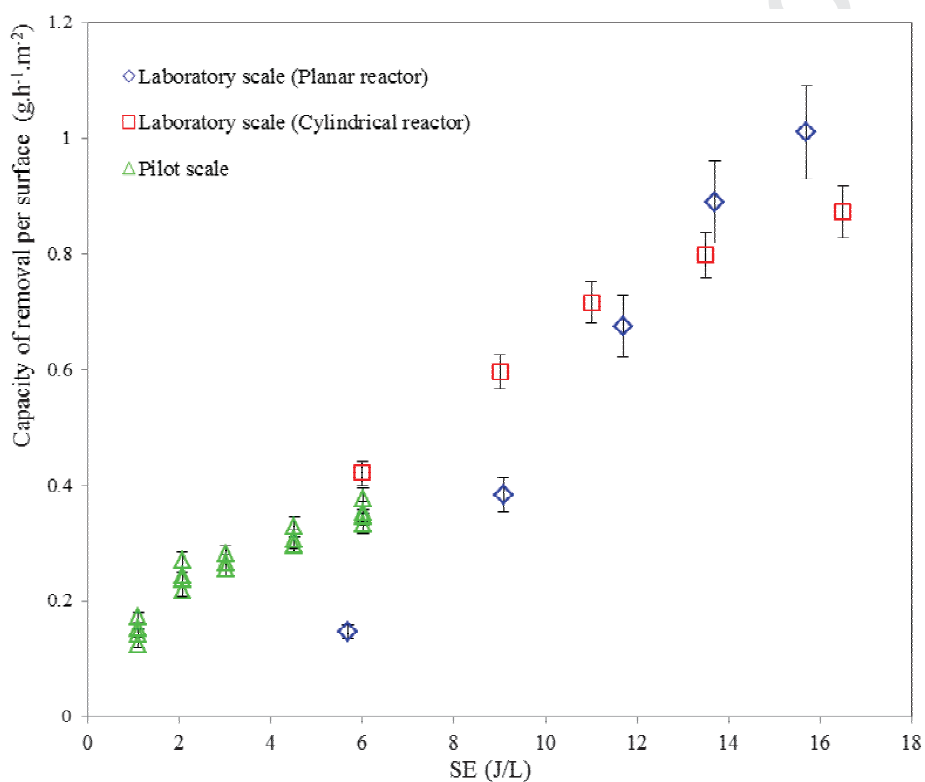
587

588

589

590

591



592

593 **Figure 8: Different reactors and scales comparison vs. specific energy: Feed of Isoval =**  
594 **1.2 g.h<sup>-1</sup>, residence time=0.6s**

595